

The Dynamical Parameters of the Universe

Matts Roos and S. M. Harun-or-Rashid

Department of Physics, Division of High Energy Physics,
University of Helsinki, Finland

ABSTRACT

The results of different analyses of the dynamical parameters of the Universe are converging towards agreement. Remaining disagreements reflect systematic errors coming either from the observations or from differences in the methods of analysis. Compiling the most precise parameter values with our estimates of such systematic errors added, we find the following best values: the baryonic density parameter $\Omega_b h^2 = 0.019 \pm 0.02$, the density parameter of the matter component $\Omega_m = 0.29 \pm 0.06$, the density parameter of the cosmological constant $\Omega_\lambda = 0.71 \pm 0.07$, the spectral index of scalar fluctuations $n_s = 1.02 \pm 0.08$, the equation of state of the cosmological constant $w_\lambda < -0.86$, and the deceleration parameter $q_0 = -0.56 \pm 0.04$. We do not modify the published best values of the Hubble parameter $H_0 = 0.73 \pm 0.07$ and the total density parameter $\Omega_0^{+0.03}_{-0.02}$.

1 INTRODUCTION

Our information on the dynamical parameters of the Universe describing the cosmic expansion comes from three different epochs. The earliest is the Big Bang nucleosynthesis which occurred a little over 2 minutes after the Big Bang, and which left its imprint in the abundances of the light elements affecting the baryonic density parameter Ω_b . The discovery of anisotropic temperature fluctuations in the cosmic microwave background radiation at large angular scales (CMBR) by COBE-DMR [1], followed by small scale anisotropies measured in the balloon flights BOOMERANG [2] and MAXIMA [3], by the radio telescopes Cosmic Background Imager (CBI) [4], Very Small Array (VSA) [5] and Degree Angular Scale Interferometer (DASI) [6] testify about the conditions in the Universe at the time of last scattering, about 350 000 years after Big Bang. The analyses of the CMBR power spectrum give information about every dynamical parameter, in particular Ω_0 and its components Ω_b , Ω_m and Ω_λ , and the spectral index n_s . For an extensive review of CMBR detectors and results, see Bersanelli et al. [7]. Very recently, also the expected fluctuations in the CMBR polarization anisotropies has been observed by DASI [8].

The third epoch is the time of matter structures: galaxy clusters, galaxies and stars. Our view is limited to the redshifts we can observe which correspond to times of a few Gyr after Big Bang. This determines the Hubble constant, successfully done by the Hubble Space Telescope (HST) [9], and the difference $\Omega_\lambda - \Omega_m$ in the dramatic supernova Ia observations by the High- z Supernova Search Team [10] and the Supernova Cosmology Project [11]. The large scale structure (LSS) and its power spectrum has been studied in the SSRS2 and CfA2 galaxy surveys [12], in the Las Campanas Redshift Survey [13], in the Abell-ACO cluster survey [14], in the IRAS PSCz Survey [15] and in the 2dF Galaxy

Redshift Survey [16],[17]. Various sets of CMBR data, supernova data and LSS data have been analyzed jointly. We shall only refer to global analyses of the now most recent CMBR power spectra and large scale distributions of galaxies.

The list of other types of observations is really very long. To mention some, there have been observations on the gas fraction in X-ray clusters [18], on X-ray cluster evolution [19], on the cluster mass function and the Ly α forest [20], on gravitational lensing [21], on the Sunyaev-Zel'dovich effect [22], on classical double radio sources [23], on galaxy peculiar velocities [24], on the evolution of galaxies and star creation versus the evolution of galaxy luminosity densities [25].

In this review we shall cover briefly recent observations and results for the dynamical parameters H_0 , Ω_b , Ω_m , Ω_λ , Ω_0 , n_s , w_λ and q_0 . In Section 2 these parameters are defined in their theoretical context, in Section 3 we turn to the Hubble parameter, and in Section 4 to the baryonic density. The other parameters are discussed in Sections 5 and 6, which are organized according to observational method: supernovae in Section 5, CMBR and LSS in Section 6. Section 7 summarizes our results.

2 THEORY

The currently accepted paradigm describing our homogeneous and isotropic Universe is based on the Robertson–Walker metric

$$ds^2 = c^2 dt^2 - dl^2 = c^2 dt^2 - R(t)^2 \left(\frac{d\sigma^2}{1 - k\sigma^2} + \sigma^2 d\theta^2 + \sigma^2 \sin^2 \theta d\phi^2 \right) \quad (1)$$

and Einstein's covariant formula for the law of gravitation,

$$G_{\mu\nu} = \frac{8\pi G}{c^4} T_{\mu\nu} . \quad (2)$$

In Eq. (1) ds is the line element in four-dimensional spacetime, t is the time, $R(t)$ is the cosmic scale, σ is the comoving distance as measured by an observer who follows the expansion, k is the curvature parameter, c is the velocity of light, and θ , ϕ are comoving angular coordinates. In Eq. (2) $G_{\mu\nu}$ is the Einstein tensor describing the curved geometry of spacetime, $T_{\mu\nu}$ is the energy-momentum tensor, and G is Newton's constant.

From these equations one derives Friedmann's equations which can be put into the form

$$\frac{\dot{R}^2 + kc^2}{R^2} = \frac{8\pi G}{3} (\rho_m + \rho_\lambda) , \quad (3)$$

$$\frac{2\ddot{R}}{R} + \frac{\dot{R}^2 + kc^2}{R^2} = -\frac{8\pi G}{c^2} (p_m + p_\lambda) . \quad (4)$$

Here ρ are energy densities, the subscripts m and λ refer to matter and cosmological constant (or dark energy), respectively; p_m and p_λ are the corresponding pressures of matter and dark energy, respectively. Using the expression for the critical density today,

$$\rho_c = \frac{3}{8\pi G} H_0^2 , \quad (5)$$

where H_0 is the Hubble parameter at the present time, one can define density parameters for each energy component by

$$\Omega = \rho / \rho_c . \quad (6)$$

The total density parameter is

$$\Omega_0 = \Omega_m + \Omega_r + \Omega_\lambda . \quad (7)$$

In what follows we shall ignore the very small radiation density parameter Ω_r . The matter density parameter Ω_m can further be divided into a cold dark matter (CDM) component Ω_{CDM} , a baryonic component Ω_b and a neutrino component Ω_ν .

The pressure of matter is certainly very small, otherwise one would observe the galaxies having random motion similar to that of molecules in a gas under pressure. Thus one can set $p_m = 0$ in Eq. (4) to a good approximation. If the expansion is adiabatic so that the pressure of dark energy can be written in the form

$$p_\lambda = w_\lambda \rho_\lambda c^2 , \quad (8)$$

and if dark energy and matter do not transform into one another, conservation of dark energy can be written

$$\dot{\rho}_\lambda + 3H\rho_\lambda(1 + w_\lambda) = 0 . \quad (9)$$

One further parameter is the deceleration parameter q_0 , defined by

$$q = -\frac{R\ddot{R}}{\dot{R}^2} = -\frac{\ddot{R}}{RH^2} . \quad (10)$$

Eliminating \ddot{R} between Eqs. (4) and (10) one can see that q_0 is not an independent parameter.

The curvature parameter k in Eqs. (1), (3) and (4) describes the geometry of space: a spatially open universe is defined by $k = -1$, a closed universe by $k = +1$ and a flat universe by $k = 0$. The curvature parameter is not an observable, but it is proportional to $\Omega_0 - 1$, so if Ω_0 is observed to be 1, the Universe is spatially flat.

3 THE HUBBLE PARAMETER

From the definition of the Hubble parameter $H = \dot{R}/R$ one sees that it has the dimension of inverse time. Thus a characteristic time scale for the expansion of the Universe is the Hubble time

$$\tau_H \equiv H_0^{-1} = 9.78h^{-1} \times 10^9 \text{yr}. \quad (11)$$

Here h is the commonly used dimensionless quantity

$$h = H_0 / (100 \text{ km s}^{-1} \text{ Mpc}^{-1}) . \quad (12)$$

The Hubble parameter also determines the size scale of the observable Universe. In time τ_H , radiation travelling with the speed of light has reached the Hubble radius

$$r_H \equiv \tau_H c = 3000h^{-1} \text{Mpc}. \quad (13)$$

Or, to put it differently, according to Hubble's non-relativistic law,

$$z = H_0 \frac{r}{c} , \quad (14)$$

objects at this distance would be expected to attain the speed of light which is an absolute limit in the theory of special relativity. However, in special relativity the redshift z is infinite for objects at distance r_H receding with the speed of light and thus unphysical. Therefore no information can reach us from farther away, all radiation is redshifted to infinite wavelengths and no particle emitted within the Universe can exceed this distance.

Our present knowledge of H_0 comes from the Hubble Space Telescope (HST) Key Project [9]. The goal of this project was to determine H_0 by a Cepheid calibration of a number of independent, secondary distance indicators, including Type Ia supernovae, the Tully-Fisher relation, the fundamental plane for elliptical galaxies, surface brightness fluctuations, and type II supernovae. Here we shall restrict the discussion to the best absolute determinations of H_0 , which are those from supernovae of type Ia.

Visible bright supernova explosions are very brief events (one month) and very rare, historical records show that in our Galaxy they have occurred only every 300 years. The most recent one occurred in 1987 (code name SN1987A), not exactly in our Galaxy but in the nearby Large Magellanic Cloud (LMC). Since it now has become possible to observe supernovae in very distant galaxies, one does not have to wait 300 years for the next one.

The physical reason for this type of explosion (type SNII supernova) is the accumulation of Fe-group elements at the core of a massive red giant star of size 8–200 M_\odot which already has burned its hydrogen, helium and other light elements. Another type of explosion (type SNIa supernova) occurs when a degenerate dwarf star of CNO composition enters a stage of rapid nuclear burning to Fe-group elements.

The SNIa is the brightest and most homogeneous class of supernovæ with hydrogen-poor spectra, their peak brightness can serve as remarkably precise standard candles visible from very far. Additional information is provided by the colour, the spectrum, and an empirical correlation observed between the time scale of the sharply rising light curve and the peak luminosity, which is followed by a gradual decline. Although supernovæ are difficult to find, they can be used to determine H_0 out to great distances, 500 Mpc or $z \approx 0.1$, and the internal precision of the method is very high. At greater distances one can still find supernovæ, but Hubble's linear law (14) is then no longer valid, the velocity starts to accelerate.

Supernovæ of type II are fainter, and show a wider variation in luminosity. Thus they are not standard candles, but the time evolution of their expanding atmospheres provides an indirect distance indicator, useful out to some 200 Mpc.

Two further methods to determine H_0 make use of correlations between different galaxy properties. Spiral galaxies rotate, and there the Tully-Fisher relation correlates total luminosity with maximum rotation velocity. This is currently the most commonly applied distance indicator, useful for measuring extragalactic distances out to about 150 Mpc. Elliptical galaxies do not rotate, they are found to occupy a "fundamental plane" in which an effective radius is tightly correlated with the surface brightness inside that radius and with the central velocity dispersion of the stars. In principle this method could be applied out to $z \approx 1$, but in practice stellar evolution effects and the non-linearity of Hubble's law limit the method to $z \lesssim 0.1$, or about 400 Mpc.

The resolution of individual stars within galaxies clearly depends on the distance to the galaxy. This method, called surface brightness fluctuations (SBF), is an indicator of relative distances to elliptical galaxies and some types of spirals. The internal precision of the method is very high, but it can be applied only out to about 70 Mpc.

Observations from the HST combining all this methods [9] and independent SNIa observations from observatories on the ground [26] agree on a value

$$H_0 = 73 \pm 2 \pm 7 \text{ km s}^{-1} \text{ Mpc}^{-1}. \quad (15)$$

Note that the second error in Eq. (15) which is systematical, is much bigger than the statistical error. This illustrates that there are many unknown effects which complicate the determination of H_0 , and which in the past have made all determinations controversial. To give just one example, if there is dust on the sight line to a supernova, its light would be reddened and one would conclude that the recession velocity is higher than it in reality is. There are other methods such as weak lensing which do not suffer from this systematic error, but they have not yet reached a precision superior to that in Eq. (15).

4 THE BARYONIC DENSITY

The ratio of baryons to photons or the baryon abundance is defined as

$$\eta \equiv \frac{N_b}{N_\gamma} \simeq 2.75 \times 10^{-8} \Omega_b h^2 \quad (16)$$

where N_b is the number density of baryons and $N_\gamma = 4.11 \times 10^8 \text{ m}^{-3}$ is the number density of photons. Thus the primordial abundances of baryonic matter in the standard Big Bang nucleosynthesis scenario (BBN) is proportional to $\Omega_b h^2$. Its value is obtained in direct measurements of the abundances of the light elements ^4He , ^3He , ^2H or D, ^7Li and indirectly from CMBR observations and galaxy cluster observations.

If the observed abundances are indeed of cosmological origin, they must not significantly be affected by later stellar processes. The helium isotopes ^3He and ^4He cannot be destroyed easily but they are continuously produced in stellar interiors. Some recent helium is blown off from supernova progenitors, but that fraction can be corrected for by observing the total abundance in hydrogen clouds of different age, and extrapolating it to time zero. The remainder is then primordial helium emanating from BBN. On the other hand, the deuterium abundance can only decrease, it is easily burned to ^3He in later stellar events. The case of ^7Li is complicated because some fraction is due to later galactic cosmic ray spallation products.

Among the light elements the ^4He abundance is easiest to observe, but also least sensitive to $\Omega_b h^2$, its dependence is logarithmic, so that only very precise measurements are relevant. The best "laboratories" for measuring the ^4He abundance are a class of low-luminosity dwarf galaxies called Blue Compact Dwarf (BCD) galaxies, which undergo an intense burst of star formation in a very compact region. The BCDs are among the most metal-deficient gas-rich galaxies known. Since their gas has not been processed during many generations of stars, it should approximate well the pristine primordial gas.

Over the years the observations have yielded many conflicting results, but the data are now progressing towards a common value [27], in particular by the work of Yu. I. Izotov and his group. The analysis in their most recent paper [28], based on the two most metal-deficient BCDs known, gives the result

$$\Omega_b(^4\text{He}) h^2 = 0.017 \pm 0.005 \quad (2\sigma \text{ CL}) , \quad (17)$$

where the error is statistical only. Usually one quotes the ratio Y_p of mass in ^4He to total mass in ^1H and ^4He , which in this case is 0.2452 with a systematic error in the positive direction estimated to be 2-4%. Because of the logarithmic dependence, this error translated to $\Omega_b h^2$ could be considerable, of the order of 100% .

The ^3He isotope can be seen in the Milky Way interstellar medium and its abundance is a strong constraint on $\Omega_b h^2$. The ^3He abundance has been determined from 14 years

of data by Balser et al. [29]. More interestingly, Bania et al. [30] combined Milky Way data with the helium abundance in stars [31] to find

$$\Omega_b(^3\text{He}) h^2 = 0.020_{-0.003}^{+0.007} \quad (1\sigma \text{ CL}) . \quad (18)$$

There are actually three different errors in their analysis, and their quadratic sum gives the total error. The first error is from the observed emission-line that includes the errors in the Gaussian fits to the observed line parameters. The second error is from the standard deviation of the observed continuum data and the third error is the percent uncertainty of all models that have been used in the analyses of reference [29].

For a constraint on $\Omega_b h^2$ from ^7Li , Coc et al. [32] update the previous work of several groups. More importantly, they include NACRE data [33] in their compilation, and the uncertainties are analysed in detail. There is some lack of information about the neutron-induced reaction in the NACRE compilation, but the main source of uncertainty for the lighter neutron-induced reaction (e.g. $^1\text{H}(n, \gamma)^2\text{H}$ and $^3\text{He}(n, p)^3\text{H}$) is the neutron lifetime (for the present value see the Review of Particle Physics [34]). However, there is no new information about the heavier neutron-induced reaction (e.g. ^7Li) or for $^3\text{He}(d, p)^3\text{He}$, but in this compilation the Gaussian errors have been opted from the polynomial fit of Nollett & Burles [35]. We quote Coc et al. [32] for

$$\Omega_b(^7\text{Li}) h^2 = 0.015 \pm 0.003 \quad (1\sigma \text{ CL}) . \quad (19)$$

The strongest constraint on the baryonic density comes from the primordial deuterium abundance. Deuterium is observed as a Lyman- α feature in the absorption spectra of high-redshift quasars. A recent analysis [36] gives

$$\Omega_b(^2\text{H}) h^2 = 0.020 \pm 0.001 \quad (1\sigma \text{ CL}) , \quad (20)$$

more precisely than any other determination. Some systematic uncertainties remain in the calculations arising from the reaction cross sections.

Very recently Chiappini et al. [37] have redefined the production and destruction of ^3He in low and intermediate mass stars. They also propose a new model for the time evolution of deuterium in the Galaxy. Taken together, they conclude that $\Omega_b h^2 \gtrsim 0.017$, in good agreement with the values in Eqs. (18) and (20).

Let us now turn to the information from the cosmic microwave background radiation and from large scale structures. There are many analyses of joint CMBR data, in particular three large compilations. Percival et al. [38] combine the data from COBE-DMR [1] MAXIMA [39], BOOMERANG [40], DASI [6], VSA [5] and CBI [4] with the 2dFGRS LSS data [17]. Wang et al. [41] combine the same CMBR data (except VSA) with 20 earlier CMBR power spectra, take their LSS power spectra from the IRAS PSCz survey [15], and include constraints from Lyman α forest spectra [42] and from the Hubble parameter [9]

quoted in Eq. (15). Sievers et al. [43] also use the same CMBR data as Percival et al.[38] (except VSA), combine them with earlier LSS data, and use the HST Hubble parameter [9] quoted in Eq. (15) and the supernova data referred to in Section 5 as supplementary constraints. All these analyses are maximum likelihood fits based on frequentist statistics, so the use of the Bayesian term "prior" for constraint is a misnomer.

Assuming that the initial seed fluctuations were adiabatic, Gaussian, and well described by power law spectra, the values of a large number of parameters are obtained by fitting the observed power spectrum. Here we shall only discuss results on $\Omega_b h^2$ which is essentially measured by the relative magnitudes of the first and second acoustic peaks in the CMBR power spectrum, returning to this subject in more detail in Section 6.

The data used in the three compilations are overlapping but not identical, and the central values show a spread over ± 0.0003 . This we treat as a systematic error to the straight unweighted average of the central values. Two compilations [38], [41] consider models with and without a tensor component. Since the fits are equally good in both cases we take their difference, ± 0.0008 , to constitute another systematic error. We shall use this averaging prescription also in Section 6 to obtain values of other parameters. All the analyses can then be summarized by the value

$$\Omega_b(\text{CMBR}) h^2 = 0.022 \pm 0.002 \pm 0.001 \quad (1\sigma \text{ CL}) , \quad (21)$$

where the statistical error corresponds to references [38], [41].

| <i>Method</i> | η | $\Omega_b h^2$ | <i>Error</i> | <i>References</i> |
|-------------------------|--|--|------------------------|-------------------|
| ^4He abundance | $4.7 \begin{smallmatrix} +1.0 \\ -0.8 \end{smallmatrix} \times 10^{-10}$ | 0.017 ± 0.005 | 2σ stat. only | [28] |
| ^3He abundance | $5.4 \begin{smallmatrix} +2.2 \\ -1.2 \end{smallmatrix} \times 10^{-10}$ | $0.020 \begin{smallmatrix} +0.007 \\ -0.003 \end{smallmatrix}$ | 1σ stat. only | [30] |
| ^7Li abundance | 5.0×10^{-10} | 0.015 ± 0.003 | 1σ stat. only | [32] |
| ^2H abundance | $5.6 \pm 0.5 \times 10^{-10}$ | 0.020 ± 0.001 | 1σ stat.+syst. | [36] |
| CMBR + 2dFGRS | — | $0.022 \pm 0.002 \pm 0.001$ | 1σ stat.+ syst. | [38][41] |

Table 1: The baryonic density parameter

In Table 1 we summarize the results from Eqs. (17-21). From this table one can conclude that all determinations are consistent with the most precise one from deuterium [36]. A weighted mean using the quoted errors yields 0.0194 ± 0.0008 which is dominated by deuterium. However, all light element abundance determinations generally suffer from the potential for systematic errors. As to CMBR, the statistical errors quoted in all compilations have been obtained by marginalizing, so they are certainly unrealistically small. We take a conservative approach and add a systematic error of ± 0.002 linearly to each of the five data values before averaging. The weighted mean is then

$$\Omega_b h^2 = 0.019 \pm 0.002 , \quad (22)$$

in excellent agreement with all the uncorrected input values in Table 1.

One further source of Ω_b information is galaxy clusters which are composed of baryonic and non-baryonic matter. The baryonic matter takes the forms of hot gas emitting X-rays, stellar mass observed in visual light, and perhaps invisible baryonic dark matter of unknown composition. Let us denote the respective fractions f_{gas} , f_{gal} , and f_{bdm} . Then

$$f_{gas} + f_{gal} + f_{bdm} = \Upsilon \frac{\Omega_b}{\Omega_m} , \quad (21)$$

where Υ describes the possible local enhancement or diminution of baryon matter density in a cluster compared to the universal baryon density. This relation could in principle be used to determine Ω_b when one knows Ω_m (or vice versa), since f_{gas} and f_{gal} can be measured, albeit with large scatter, while f_{bdm} can be assumed negligible. Cluster formation simulations give information on Υ [44],[45] to a precision of about 10%. However, the precision obtained for $\Omega_b h^2$ by adding several 10% errors in quadrature does not make this method competitive.

5 SUPERNOVA Ia CONSTRAINTS

In Section 3 we already mentioned briefly the physics of supernovæ. The SN Ia observations by the High-z Supernova Search Team (HSST) [10] and the Supernova Cosmology Project (SCP) [11] are well enough known not to require a detailed presentation here. The importance of these observations lies in that they determine approximately the linear combination $\Omega_\lambda - \Omega_m$ which is orthogonal to $\Omega_0 = \Omega_m + \Omega_\lambda$, see Figure 1.

HSST use two quite distinct methods of light-curve fitting to determine the distance moduli of their 16 SNe Ia studied. Their luminosity distances are used to place constraints on six cosmological parameters: h , Ω_m , Ω_λ , q_0 , and the dynamical age of the Universe, t_0 . The MLCS method involves statistical methods at a more refined level than the empirical template model. The distance moduli are found from a χ^2 analysis using an empirical model containing four free parameters. The MLCS method and the template method give moduli which differ by about 1σ . Once the distance moduli are known, the parameters h , Ω_m , Ω_λ are determined by a maximum likelihood fit, and finally the Hubble parameter is integrated out. (The results are really independent of h .) One may perhaps be somewhat concerned about the assumption that each modulus is normally distributed. We have no reason to doubt that, but if the iterative χ^2 analysis has yielded systematically skewed pdf's, then the maximum likelihood fit will amplify the skewness.

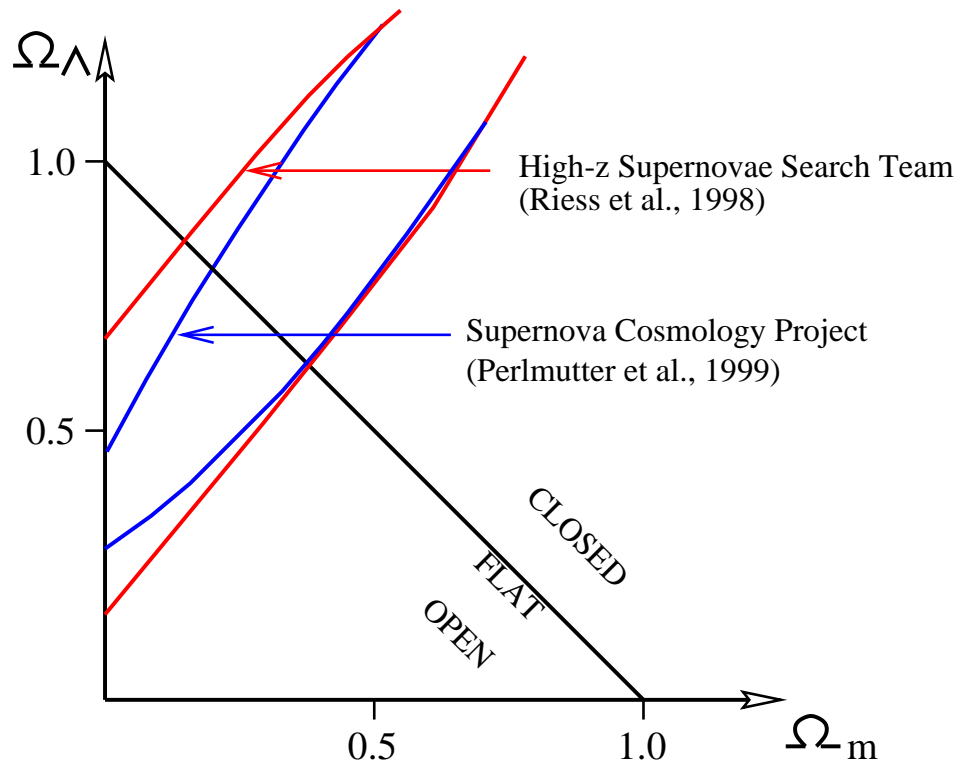


Figure 1: The best fit confidence regions in $(\Omega_m - \Omega_\Lambda)$ plane in the analyses of the Supernova Cosmology Project (blue curves) [11] and the High Redshift Supernova Search Team (red curves) [10]. The diagonal line corresponds to a flat cosmology. Above the flat line the Universe is closed and below it is open.

The authors state that "the dominant source of statistical uncertainty is the extinction measurement". The main doubt raised about the SNe Ia observations is the risk that (part of) the reddening of the SNe Ia could be caused by intervening dust rather than by the cosmological expansion, as we already noted after Eq. (15). Among the possible systematic errors investigated is also that associated with extinction. No systematic error is found to be important here, but for such a small sample of SNe Ia one can expect that the selection bias might be the largest problem.

The authors do not express any view about which method should be considered more reliable, thus noting that "we must consider the difference between the cosmological constraints reached from the two fitting methods to be a systematic uncertainty". We shall come back to this question later. Here we would like to point out that if one corrects for the unphysical region $\Omega_m < 0$ using the method of Feldman & Cousins [46], the best value and the confidence contours will be shifted slightly towards higher values of Ω_0 . This shift will be more important for the MLCS method than for the template method, because the former extends deeper into the unphysical Ω_m region.

Let us now turn to SCP, which studied 42 SNe Ia. The MLCS method described above is basically repeated, but modified in many details for which we refer the reader to the source [11]. The distance moduli are again found from a χ^2 analysis using an empirical model containing four free parameters, but this model is slightly different from the HSST treatment. The parameters Ω_m and Ω_λ are then determined by a maximum likelihood fit to four parameters, of which the parameters \mathcal{M}_B (an absolute magnitude) and α (the slope of the width-luminosity relation) are just ancillary variables which are integrated out (it does not enter at all). The likelihood contours in $(\Omega_m - \Omega_\lambda)$ plane of both supernovae projects (SCP and HSST) are shown in Figure-1. The authors then correct the resulting likelihood contours for the unphysical region $\Omega_m < 0$ using the method of Feldman & Cousins [46]. Since the number of SNe Ia is here so much larger than in HSST, the effects of selection and of possible systematic errors can be investigated more thoroughly. SCP quotes a total possible systematic uncertainty to Ω_m^{flat} and Ω_λ^{flat} of 0.05.

If we compare the observations along the line defining a flat Universe, SCP finds $\Omega_\lambda - \Omega_m = 0.44 \pm 0.085 \pm 0.05$, whereas HSST finds $\Omega_\lambda - \Omega_m = 0.36 \pm 0.10$ for the MLCS method and $\Omega_\lambda - \Omega_m = 0.68 \pm 0.09$ for the template method. Treating this difference as a systematic error of size ± 0.16 the combined SCP result is $0.52 \pm 0.10 \pm 0.16$. SCP and HSST then agree within their statistical errors – how well they agree cannot be established since they are not completely independent. We choose to quote a combined HSST and SCP value

$$\Omega_\lambda - \Omega_m = 0.5 \pm 0.1, \quad (22)$$

which excludes a flat de Sitter universe with $\Omega_\lambda - \Omega_m = 1$ by 5σ , and excludes a flat Einstein – de Sitter universe with $\Omega_\lambda - \Omega_m = -1$ by 10σ .

6 CMBR AND LSS CONSTRAINTS

The most important source of information on the cosmological parameters are the anisotropies observed in the CMBR temperature and polarization maps over the sky. The temperature angular power spectrum has been measured and analyzed since 1992 [1], whereas the polarization spectrum is very recent [8] and has not yet been analyzed to obtain values for the dynamical parameters. Given the temperature angular power spectrum, the polarization spectrum is predicted with essentially no free parameters. At the moment one can say that the temperature angular power spectrum supports the current model of the Universe as defined by the dynamical parameters obtained from the temperature angular power spectrum.

Temperature fluctuations in the CMBR around a mean temperature in a direction α on the sky can be analyzed in terms of the autocorrelation function $C(\theta)$ which measures the average product of temperatures in two directions separated by an angle θ ,

$$C(\theta) = \left\langle \frac{\delta T}{T}(\alpha) \frac{\delta T}{T}(\alpha + \theta) \right\rangle . \quad (23)$$

For small angles (θ) the temperature autocorrelation function can be expressed as a sum of Legendre polynomials $P_\ell(\theta)$ of order ℓ , the wave number, with coefficients or powers a_ℓ^2 ,

$$C(\theta) = \frac{1}{4\pi} \sum_{\ell=2}^{\infty} a_\ell^2 (2\ell + 1) P_\ell(\cos \theta) . \quad (24)$$

All analyses start with the quadrupole mode $\ell = 2$ because the $\ell = 0$ monopole mode is just the mean temperature over the observed part of the sky, and the $\ell = 1$ mode is the dipole anisotropy due to the motion of Earth relative to the CMBR. In the analysis the powers a_ℓ^2 are adjusted to give a best fit of $C(\theta)$ to the observed temperature. The resulting distribution of a_ℓ^2 values versus ℓ is the power spectrum of the fluctuations, see Figure 2. The higher the angular resolution, the more terms of high ℓ must be included.

The exact form of the power spectrum is very dependent on assumptions about the matter content of the Universe. It can be parametrized by the vacuum density parameter $\Omega_k = 1 - \Omega_0$, the total density parameter Ω_0 with its components Ω_m , Ω_λ , and the matter density parameter Ω_m with its components Ω_b , Ω_{CDM} , Ω_ν . Further parameters are the Hubble parameter h , the tilt of scalar fluctuations n_s , the CMBR quadrupole normalization for scalar fluctuations Q , the tilt of tensor fluctuations n_t , the CMB quadrupole normalization for tensor fluctuations r , and the optical depth parameter τ . Among these parameters, really only about six have an influence on the fit.

In Section 4 we already noted that the relative magnitudes of the first and second acoustic peaks are sensitive to Ω_b . The position of the first acoustic peak in multipole ℓ - space is sensitive to Ω_0 , which makes the CMBR information complementary (and in Ω_m , Ω_λ - space orthogonal) to the supernova information. A decrease in Ω_0 corresponds to a decrease in curvature and a shift of the power spectrum towards high multipoles. An increase in Ω_λ (in flat space) and a decrease in h (keeping $\Omega_b h^2$ fixed) both boost the peaks and change their location in ℓ - space.

Let us now turn to the distribution of matter in the Universe which can, to some approximation, be described by the hydrodynamics of a viscous, non-static fluid. In such a medium there naturally appear random fluctuations around the mean density $\bar{\rho}(t)$, manifested by compressions in some regions and rarefactions in other regions. An ordinary fluid is dominated by the material pressure, but in the fluid of our Universe three effects are competing: radiation pressure, gravitational attraction and density dilution due to the Hubble flow. This makes the physics different from ordinary hydrodynamics, regions of overdensity are gravitationally amplified and may, if time permits, grow into large inhomogeneities, depleting adjacent regions of underdensity.

Two complementary techniques are available for theoretical modelling of galaxy formation and evolution: numerical simulations and semi-analytic modelling. The strategy in both cases is to calculate how density perturbations emerging from the Big Bang turn into visible galaxies. This requires following through a number of processes: the growth of dark matter halos by accretion and mergers, the dynamics of cooling gas, the transformation of cold gas into stars, the spectrophotometric evolution of the resulting stellar populations, the feedback from star formation and evolution on the properties of prestellar gas, and the build-up of large galaxies by mergers.

As in the case of the CMBR, an arbitrary pattern of fluctuations can be mathematically described by an infinite sum of independent waves, each with its characteristic wavelength λ or comoving wave number k and its amplitude δ_k . The sum can be formally expressed as a Fourier expansion for the density contrast at comoving spatial coordinate \mathbf{r} and world time t ,

$$\delta(\mathbf{r}, t) \propto \sum \delta_k(t) e^{i\mathbf{k}\cdot\mathbf{r}} , \quad (25)$$

where \mathbf{k} is the wave vector.

Analogously to Eq. (23) a density fluctuation can be expressed in terms of the dimensionless mass autocorrelation function

$$\xi(r) = \langle \delta(\mathbf{r}_1) \delta(\mathbf{r} + \mathbf{r}_1) \rangle \propto \sum \langle |\delta_k(t)|^2 \rangle e^{i\mathbf{k}\cdot\mathbf{r}} . \quad (26)$$

which measures the correlation between the density contrasts at two points \mathbf{r} and \mathbf{r}_1 . The powers $|\delta_k|^2$ define the power spectrum of the rms mass fluctuations,

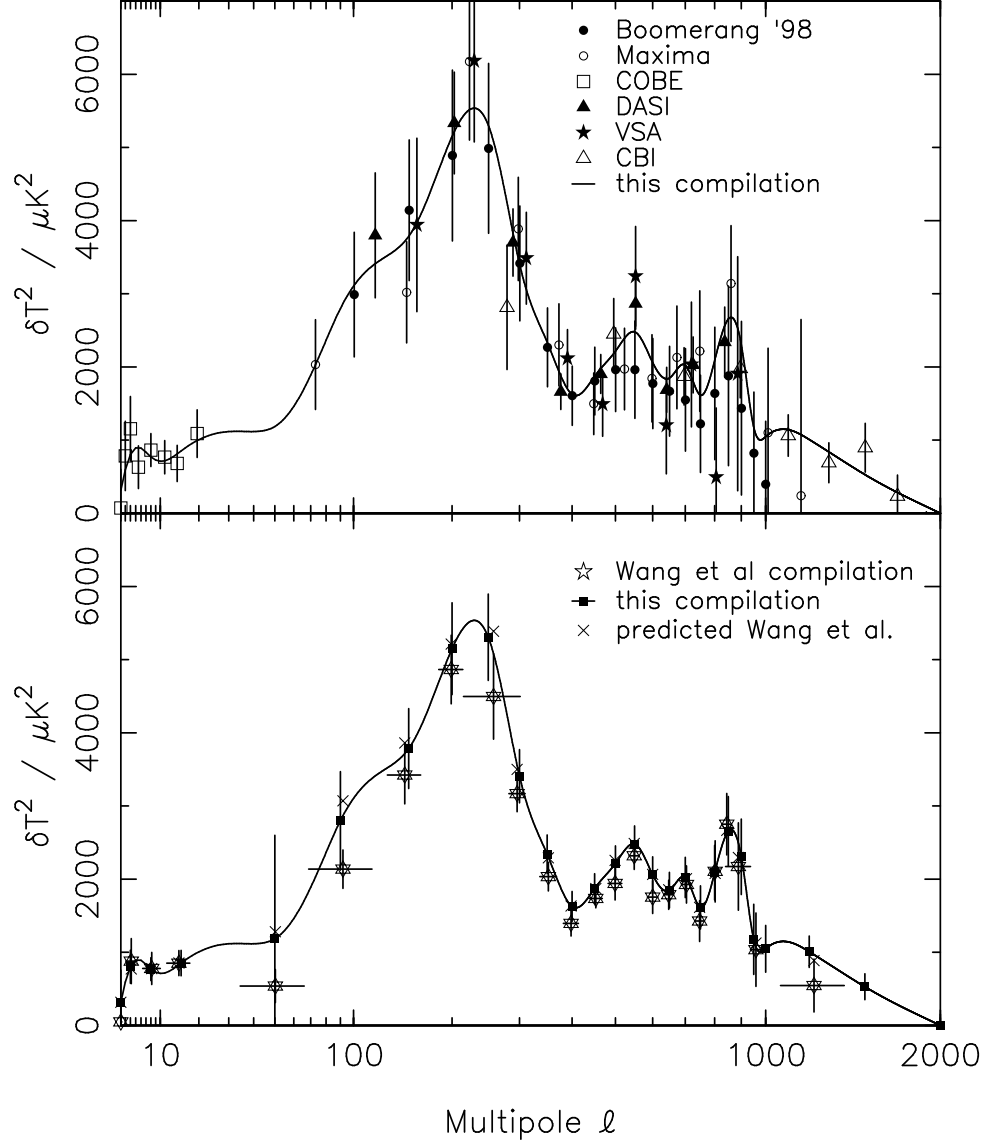


Figure 2: Top panel: a compilation of recent CMB data [38]. The solid line shows the result of a maximum-likelihood fit to the power spectrum allowing for calibration and beam uncertainty errors in addition to intrinsic errors. Bottom panel: the solid line is as above, the solid squares [38] and the crosses [41] give the points at which the amplitude of the power spectrum was estimated. For details, see reference [38].

$$P(k) = \langle |\delta_k(t)|^2 \rangle . \quad (27)$$

Thus the autocorrelation function $\xi(r)$ is the Fourier transform of the power spectrum. This is similar to the situation in the context of CMB anisotropies where the waves represented temperature fluctuations on the surface of the surrounding sky, and the powers a_ℓ^2 were coefficients in the Legendre polynomial expansion Eq. (24).

With the lack of more accurate knowledge of the power spectrum one assumes for simplicity that it is specified by a power law

$$P(k) \propto k^{n_s} , \quad (28)$$

where n_s is the spectral index of scalar fluctuations. Primordial gravitational fluctuations are expected to have an equal amplitude on all scales. Inflationary models also predict that the power spectrum of matter fluctuations is almost scale-invariant as the fluctuations cross the Hubble radius. This is the Harrison–Zel’dovich spectrum, for which $n_s = 1$ ($n_s = 0$ would correspond to white noise).

Since fluctuations in the matter distribution has the same primordial cause as CMBR fluctuations, we can get some general information from CMBR. There, increasing n_s will raise the angular spectrum at large values of ℓ with respect to low ℓ . Support for $\ell \approx 1.0$ come from all the available analyses: combining the results of references [38], [41], [43] by the averaging prescription in Section 4, we find

$$n_s = 1.02 \pm 0.06 \pm 0.05 . \quad (29)$$

Phenomenological models of density fluctuations can be specified by the amplitudes δ_k of the autocorrelation function $\xi(r)$. In particular, if the fluctuations are Gaussian, they are completely specified by the power spectrum $P(k)$. The models can then be compared to the real distribution of galaxies and galaxy clusters, and the phenomenological parameters determined.

As we noted in Section 4, there are several joint compilations of CMBR power spectra and LSS power spectra of which we are interested in the three largest ones [38], [41], [43]. Combining their results for Ω_m by the averaging prescription in Section 4, we find

$$\Omega_m = 0.29 \pm 0.05 \pm 0.04 . \quad (30)$$

If the Universe is spatially flat so that $\Omega_0 = 1$, this gives immediately the value $\Omega_\lambda = 0.71$ with slightly better precision than above. To check this assumption we can quote reference [43] from their Table 5 where they use all data,

$$\Omega_0 = 1.00 \pm \begin{smallmatrix} 0.03 \\ 0.02 \end{smallmatrix} . \quad (31)$$

Note, however, that this result has been obtained by marginalizing over all other parameters, thus its small statistical errors are conditional on n_s , Ω_m , Ω_b being anything, and we have no prescription for estimating a systematic error.

A value for Ω_λ can be found by adding $\Omega_\lambda - \Omega_m$ in Eq. (22) to Ω_m , thus $\Omega_\lambda = 0.79 \pm 0.12$. A better route appears to be to combine Eqs. (30) and (31) to give

$$\Omega_\lambda = 0.71 \pm 0.07 . \quad (32)$$

Still a third route is to add Ω_0 and $\Omega_\lambda - \Omega_m$, or to subtract them, respectively. Then one obtains

$$\Omega_m = 0.25 \pm 0.05 , \quad \Omega_\lambda = 0.75 \pm 0.05 .$$

The routes making use of $\Omega_\lambda - \Omega_m$ from Eq. (22) are, however, making multiple use of the supernova information, so we discard them.

Before ending this Section, we can quote values also for w_λ and q_0 . The notation here implies that w_λ is taken as the equation of state of a quintessence component, so that its value could be $w_\lambda > -1$. The equation of state of a cosmological constant component is of course $w_\lambda = -1$. In a flat universe w_λ is completely correlated to Ω_λ and therefore also to Ω_m .

We choose to quote the analysis by Bean and Melchiorri [47] who combine CMBR power spectra from COBE-DMR [1], MAXIMA [39], BOOMERANG [40], DASI [6], the supernova data from HSST [10] and SCP [11], the HST Hubble constant [9] quoted in Eq. (15), the baryonic density parameter Ω_b $h^2 = 0.020 \pm 0.005$ and some LSS information from local cluster abundances. They then obtain likelihood contours in the w_λ, Ω_m space from which they quote the 1σ bound $w_\lambda < -0.85$. If we permit ourselves to restrict their confidence range further by using our value $\Omega_m = 0.29 \pm 0.06$ from Eq. (30), the result is changed only slightly to

$$w_\lambda < -0.86 , \quad (1\sigma \text{ CL}) \quad (33).$$

Finally, the deceleration parameter is not an independent quantity, it can be calculated from

$$q_0 = \frac{1}{2}\Omega_m - \Omega_\lambda = \frac{3}{2}\Omega_m - \Omega_0 = -0.56 \pm 0.04 . \quad (34)$$

The error is so small because the Ω_m and the Ω_λ errors are completely anticorrelated. Note that the negative value implies that the expansion of the Universe is accelerating.

| <i>Parameters</i> | <i>Values</i> | <i>References</i> |
|-------------------|-----------------------|-------------------|
| H_0 | 73 ± 7 | [9] |
| $\Omega_b h^2$ | 0.019 ± 0.002 | our compilation |
| Ω_m | 0.29 ± 0.06 | our compilation |
| Ω_λ | 0.71 ± 0.07 | our compilation |
| Ω_0 | $1.0^{+0.03}_{-0.02}$ | [43] |
| n_s | 1.02 ± 0.08 | our compilation |
| w_λ | < -0.86 | our compilation |
| q_0 | -0.56 ± 0.04 | our compilation |

Table 2: Best values of the dynamical parameters. The errors include 1σ statistical errors and our estimates of systematic errors, except for Ω_0 which is statistical only. The Hubble constant H_0 is given in units of $\text{km s}^{-1}\text{Mpc}^{-1}$

7 SUMMARY

Information on the dynamical parameters of the Universe are coming from the Big Bang nucleosynthesis, from the fluctuations in the temperature and polarization of the cosmic microwave background radiation, from the large scale structures of galaxies, from supernova observations and from many other cosmological effects that may not yet be of interesting precision. The results of different analyses are now converging towards agreement when in the past disagreements of the order of 100% have been known.

In this review we have taken the attitude that remaining disagreements reflect systematic errors coming either from the observations or from differences in the methods of analysis. We have then compiled the most precise parameter values, combined them and added our estimates of such systematic errors. This we have done for the baryonic density parameter $\Omega_b h^2$, the density parameter of the matter component Ω_m , the density parameter of the cosmological constant Ω_λ , the spectral index of scalar fluctuations n_s , the equation of state of the cosmological constant w_λ , and the deceleration parameter q_0 . In addition we quote the best values of the Hubble parameter H_0 and the total density parameter Ω_0 from other sources. In Table 2 we summarize our results.

The conclusion is not new: that the Universe is spatially flat, that some 25% of gravitating matter is dark and unknown, and that some 70% of the total energy content is dark, possibly in the form of a cosmological constant.

Acknowledgements: S. M. H. is indebted to the Magnus Ehrnrooth Foundation for support.

References

- [1] G. F. Smoot et al., 1992, ApJ 396, L1
- [2] P. de Bernardis et al., 2000, Nature 404, 955
- [3] A. Balbi et al., 2000, ApJ 545, L1; S. Hanany et al., 2000, ApJ 545, L5
- [4] T. J. Pearson et al., 2002, astro-ph/0205388; B. S. Mason et al., 2002, astro-ph/0205384
- [5] P. E. Scott et al., 2002, astro-ph/0205380
- [6] N. W. Halverson et al., 2002, ApJ 568, 38; C. Pryke et al., 2002, ApJ 568, 46
- [7] M. Bersanelli, D. Maino & A. Mennella, 2002, astro-ph/0209215, Submitted to “La Rivista del Nuovo Cimento”.
- [8] J. Kovac et al., 2002, astro-ph/0209478
- [9] W. L. Freedman et al., 2001, ApJ 553, 47
- [10] A. G. Riess et al., 1998, AJ 116, 1009
- [11] S. Perlmutter et al., 1998, Nature 391, 51; 1999, ApJ 517, 565
- [12] L. N. da Costa et al., 1994, ApJ 424, L1
- [13] S. A. Shectman et al., 1996, ApJ 470, 172
- [14] J. Retzlaff et al., 1998, New Astron. A3, 631
- [15] W. Saunders et al., 2000, MNRAS 317, 55
- [16] J. A. Peacock et al., 2001, Nature 410, 169
- [17] M. Colless et al., 2001, MNRAS 328, 1039
- [18] A. E. Evrard, 1997, MNRAS 292, 289
- [19] N. A. Bahcall & X. Fan, 1998, ApJ 504, 1; V. R. Eke et al., 1998, MNRAS 298, 1145
- [20] D. H. Weinberg et al., 1999, ApJ 522, 563
- [21] M. Chiba & Y. Yoshii, 1999, ApJ 510, 42; P. Helbig, 2000, Proceedings IAU 201, astro-ph/0011031; M. Im, R. E. Griffiths & K. U. Ratnatunga, 1997, ApJ 475, 457

- [22] M. Birkinshaw 1999, Phys. Rept. 310, 97; J. E. Carlstrom, G. P. Holder and E. D. Reese, 2002, astro-ph/0208192
- [23] E. J. Guerra, R. A. Daly & L. Wan, 2000, ApJ 544, 659
- [24] I. Zehavi & A. Dekel, 1999, Nature 401, 252
- [25] T. Totani, 1997, IAU proceedings, Kyoto, Japan, astro-ph/9710312
- [26] B. K. Gibson & C. B. Brook, 2000, astro-ph/0011567; 2001, ASP Conference Services, 666
- [27] V. Luridiana, 2002, astro-ph/0209177; to appear in Proc. XXXVIIth Moriond Astrophys. Meeting "The Cosmological Model", Les Arcs, France, March 16-23, 2002
- [28] T. X. Thuan & Y. I. Izotov, 2001, astro-ph/0112348; to appear in "Matter in the Universe", ed P. Jetzer, K. Pretzl and R. von Steiger, Kluwer, Dordrecht (2002)
- [29] D. S. Balser et al., 1999, ApJ 522, L73; 1999, ApJ 510, 759
- [30] T. M. Bania, R. T. Rood & D. S. Balser, 2002, Nature 415, 54
- [31] C. Charbonnel, 1995, ApJ 453, L41; C. Charbonnel et al., 1998, A & A 332, 204; 1998, A & A 336, 915; 1998, Space Sci. Rev. 84, 199
- [32] A. Coc et al., 2002, PR D65, 043510
- [33] C. Angulo et al., 1999, Nucl. Phys. A656, 3
- [34] D. E. Groom et al., 2000, Eur. Phys. J. C15, 1
- [35] K. M. Nollett & S. Burles, 2000, PR D61, 123505; 2001, ApJ 552, L1
- [36] S. Burles, K. M. Nollett & M. S. Turner, 2001, ApJ 552, L1
- [37] C. Chiappini, A. Renda & F. Matteucci, 2002, astro-ph/0209240 and A & A (accepted)
- [38] W. J. Percival et al., 2002, astro-ph/0206256; 2001, MNRAS 327, 1297
- [39] A. T. Lee et al., 2001, ApJ 561, L1
- [40] C. B. Netterfield et al., 2002, ApJ 571, 604
- [41] X. Wang, M. Tegmark & M. Zaldarriaga, 2002, PR D65, 123001
- [42] A. C. Croft et al., 2002, ApJ (December 10 issue), astro-ph/0012324

- [43] J. L. Sievers et al., 2002, astro-ph/0205387
- [44] V. R. Eke, J. F. Navarro, & C. S. Frenk, 1998, ApJ, 503, 569
- [45] C. S. Frenk et al., 1999, ApJ 525, 554
- [46] G. J. Feldman & R. D. Cousins, 1998, PR D57, 3873
- [47] R. Bean & A. Melchiorri, 2002, PR D65, 041302